

# EEG Arousal Detection using SVM and EMD based Frequency Detection Method

**U.S.B.K.Mahalaxmi**

*Research Scholar, Department of Instrument Technology,  
Andhra University, Visakhapatnam, Andhra Pradesh, India.  
Orcid Id: 0000-0002-1472-7185*

**M.Ramesh Patnaik**

*Sr. Assistant Professor, Department of Instrument Technology,  
Andhra University, Visakhapatnam, Andhra Pradesh, India.  
Orcid Id: 0000-0001-7543-1831*

## Abstract

Arousals in sleep are the reason behind sleep fragmentation which is detectable using the electroencephalographic (EEG) signals. As it requires a lot of time, automatization methods are essential. In this paper, arousal detection technique is presented using two phases; signal processing and machine learning algorithms. In the first phase, arousal related events are acknowledged in the EEG signals and in the electromyography (EMG). In the wake of disposing of those events that don't meet the mandatory features, the subsequent set is utilized to extricate numerous parameters. In the second phase, Support Vector Machines (SVM) are tuned with these parameters. The work has been compared with ground truth defined in dataset. The proposed model shows an accuracy of 90.44%, False Negative Rate of 42.6471 and a False Positive Rate of 8.2564 in the arousal events detection.

The another approach to justify the adaptive frame of EEG data, EMD approach is developed along with DWT based band filtration. The different band of data is extracted with DWT and further EMD is applied to get different IMFs. These IMFs gives the micro information about frequency. A differential equation based frequency detection approach has been defined to detect the change in frequency according to AASM. The developed prototype is compared with ground truth attributes for arousal index given in dataset and found very similar detection with some variation of duration of Arousal event.

**Keywords:** AASM, EMD, EEG, EMG, IMF, PSG, REM, SVM.

## INTRODUCTION

The electroencephalographic arousal is characterized by the American Academy of Sleep Medicine (AASM), as a sudden move in electroencephalogram (EEG) frequency, containing

alpha, theta, as well as frequencies more noteworthy than 16 Hz, enduring no less than 3 seconds and with no less than 10 seconds of past constant sleep [1].

Moreover, within the Rapid Eye Movement (REM) stage, a simultaneous increment in the EMG, enduring minimum 1 second, is required. Since the fragmented sleep is caused by arousals, the sleep readings must recognize those events. Sleep contemplates are accomplished with a polysomnography (PSG), electrophysiological, pneumological and relevant data. A specialist doctor can watch the EEG and EMG derivations to identify arousals. Subsequently the recording of a PSG last an entire night, the measure of information is tremendous, making the identification of EEG arousals an extremely tedious undertaking. Subsequently, automatic identification and investigation is preferred.

Recently, various techniques attempted to take care of this issue with several methodologies, featuring the proposition of Alvarez-Estevéz et al. [2], as is situated in the utilization of machine learning models in the wake of handling one EMG and two EEG inferences, and it is the method utilized in this research work. Scoring arousals depends on ASDA (American Sleep Disorders Association) criteria [3].

The scoring of EEG arousals is autonomous from the scoring of sleep stages (i.e. an arousal can be scored in an age of recording which would be named wake by R and K criteria [4]). An arousal can continue to the wake arrange or can be trailed by an arrival to sleep.

## CHARACTERIZATION OF AROUSALS

An EEG arousal is a sudden move in EEG frequency, which may incorporate alpha and additionally theta waves or potentially delta waves as well as frequencies more noteworthy than 16 Hz enduring not less than 3 seconds, and

beginning after at least 10 persistent seconds of sleep [5] [6]. (Figures 1a and 1b)

Artifacts, K buildings and delta waves are incorporated into meeting the 3 seconds span criteria just when they happen inside the EEG frequency shift.

- A "K" complex happening instantly preceding the EEG move is excluded in the arousal length portions of the EEG completely darkened by EMG antiquity are viewed as an arousal if the adjustment in contextual EEG notwithstanding the zone clouded by EMG is at any rate > 3 seconds.
- Alpha action of under 3 seconds length in Non-REM sleep at a rate more than one burst for every 10 second is not recorded as an EEG arousal.
- Furthermore, 3 seconds of alpha sleep is not recorded as an arousal except a 10 seconds scene of alpha free sleep goes before this.
- On the off chance that both focal EEGs are equal and interpretable, the arousal must be seen in the two channels. In the event that saw in just a single of two proportional channels, the adjustment in EEG is thought to be artifact and not an arousal.
- Arousal enduring more than 15 seconds comprising conscious EEG inside a period make the period be delegated as AWAKE.

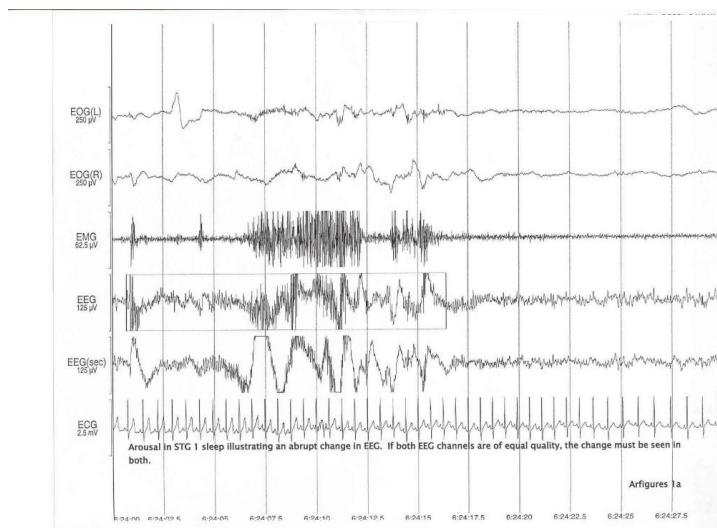


**Figure 1(a):** Sample Arousals [21]

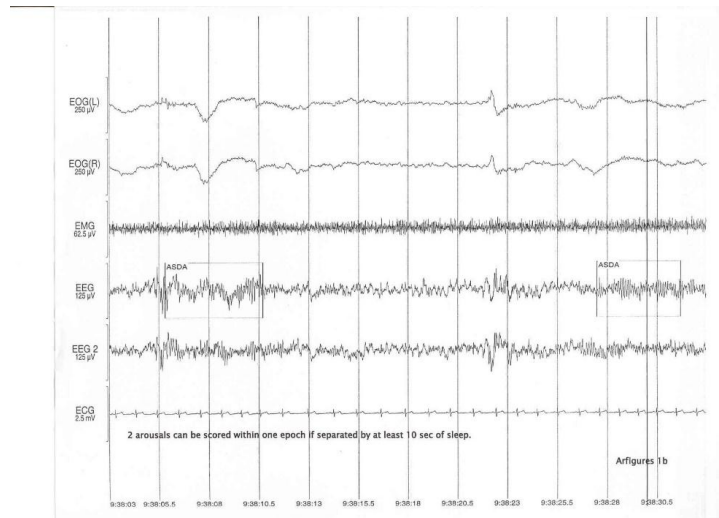


**Figure 1(b):** Sample Arousals [21]

### Common tips for Arousals

- Whenever uncertain if change in contextual EEG speaks to an unexpected change, take a gander at a 60 sec period and note if there is a discrete change from contextual EEG.
- Be mindful so as to recognize an expansion in EEG frequency from EMG artifact.
- Disconnected blasts of delta action or sawtooth like waves don't constitute an arousal. Conversely, slow waves [7] fused with quick action that varies from contextual do succeed as arousals.
- Incidentally, EEG signal is superimposed on slower waves. The moderating might be an antiquity auxiliary to development or burst of delta waves [8].

### Potential Problems

A few examinations with greater respiratory disturbance index (RDI) have numerous arousals that may seem to last > 15 sec. inside given period. On the off chance that every such period were delegated AWAKE, at that point the respiratory occasions would not be incorporated into the RDI and the RDI will be thought little of. At the point when confronted with this circumstance, the scorer may endeavor to keep the span of the arousal to as short as attainable (e.g., comparing to the extent of the waking EEG in that period). This will boost the quantity of periods comprising arousals that are caught as "SLEEP".

## PROPOSED METHOD

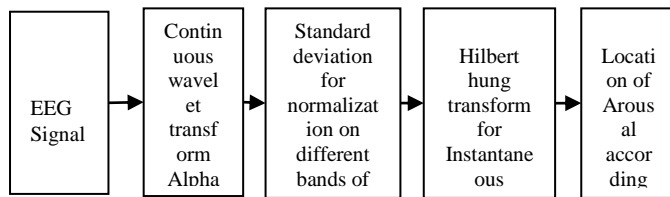


**Figure 2:** Proposed method for arousal detection

The above figure elaborates the flow for automatic detection of arousals in EEG data. The EEG sample is passed through different level of wavelet decomposition, to get various desired bands of frequency. This can be achieved with help of Butterworth filter also, but wavelet can be used for artifacts filtration using soft and hard thresholding. As well it gives more precise local representation. This paper is not focused for artifact removal situation, data is considered as artifacts free. Different bands from wavelet decomposition is further decomposed through Hilbert transform to get different IMF, every band may have different number of IMFS depends upon the frequency. Further abrupt frequency change point is detected according to time frame defined by AASM. According to rule defined by AASM detected point can be considered as Arousal index.

The degree of vigilance of an individual can be quantified by the analysis of EEG, signal which represent the electrical activity of the brain and are measured using electrodes placed on the subject's skull. These signals are composed of different types of waves that translate certain physiological states [9]:

- Delta (0.5 - 4 Hz): They are characteristic of deep sleep.
- Theta (4 - 8 Hz): They appear mostly during sleep.
- Alpha (8 - 13 Hz): They appear on adults under relaxation conditions and mental inactivity
- Beta (13 - 30 Hz): They are more pronounced during voltage states and attention.

The first signs of falling asleep usually result in the appearance alpha waves and, more rarely, theta.

### The Wavelet Transform

#### Principle of decomposition

The wavelet transform has established itself as a powerful and dignified technique interest. It is a time - scale representation that allows to describe the evolution of the characteristics of a signal in relation to an observation scale given.

$$C(a, b) = |a|^{-1/2} \int_{-\infty}^{\infty} s(t) \times \bar{\Psi}\left(\frac{t-b}{a}\right) dt \quad (1)$$

Where  $\psi(t)$  represents the mother wavelet,  $b$  is the translation parameter and the parameter of scale ( $a \neq 0$ ). The wavelet

coefficient  $C(a, b)$  of a signal  $S(t)$  depends on the shape of this signal at neighbourhood of time  $b$ . When  $S(t)$  varies little over time, its product by the wavelet  $\Psi$  generates a small area, in other words,  $C(a, b)$  is small. When, on the contrary, the sequence of the signal is irregular and that its frequency variations are comparable to that of the wavelet, the area of the product between the signal and the wavelet is important [10].

The wavelet can be interpreted as a central frequency bandpass filter  $f_c$ . The value of the coefficients is all the greater as the frequency of the analyzed signal coincides with that of the wavelet. The variation of the parameter 'a' makes it possible to determine the modes of the signal which correspond to the frequency  $f_s$  [11]:

$$f_s = f_c / a \quad (2)$$

Wavelet transform (WT) temporal resolution in the analysis of high-frequency components and the frequency resolution during the analysis of the low frequency components [12].

The wavelet transform is said to be continuous when the parameters of expansion and translation ( $a, b$ ) varies continuously [10]. It is said to be discrete when these parameters take only a few specific values. Several algorithms have been developed for the discrete transform: They take into account the principle uncertainty, using fewer values for  $b$  in the low frequencies than in the high frequencies, in order to reduce the calculation time. Before carrying out a wavelet analysis, it is necessary to choose the analyzing function (The mother wavelet) [13]. The shape of the wavelet is important, but it is important the duration and the bandwidth, these parameters determining the resolutions of the transforms in time and frequencies.

The cubic B-Spline wavelet makes it possible to make a continuous transformation of the signals and to access a temporal location of near-optimum frequencies [14]. The cubic B-Spline wavelet is expressed by.

$$\psi(t) = \frac{4k^{n+1}}{\sqrt{2\pi(n+1)}} \sigma \cos(2\pi f_0(2t - 1)) \cdot \exp\left(\frac{(2t-1)^2}{2\sigma^2(n+1)}\right) \quad (3)$$

Where  $n = 3$ ,  $k = 0.6971$ ,  $f_0 = 0.4092$ ,  $\sigma = 0.5611$ .

The cubic B-Spline wavelet is a non-orthogonal polynomial function with support compact, which allows the inverse transformation. This wavelet converges towards modulated Gaussian function. The error of approximation of a signal by the decomposition in coefficients of this wavelet is less than 3%. Another advantage is that of its representation which facilitates the implementation of the computation by an algorithm of fast transformation into discrete wavelets.

### Time-Frequency Analysis

Spectral analysis based on Fourier Transform (FT), provides good description of stationary and pseudo-stationary signals, but limitations when the signals to be analyzed are not stationary. In this the solution would be to be able to calculate their spectrum with each sample of the signal. If the signal to be studied is non-stationary, the idea of the Fourier Transform on window (STFT for Short Time Fourier Transform) is to analyze it on fractions assumed to be stationary. Each fraction of the signal is transformed using the Fourier transform, thus permitting a stepwise determination of the frequency properties of the signal.

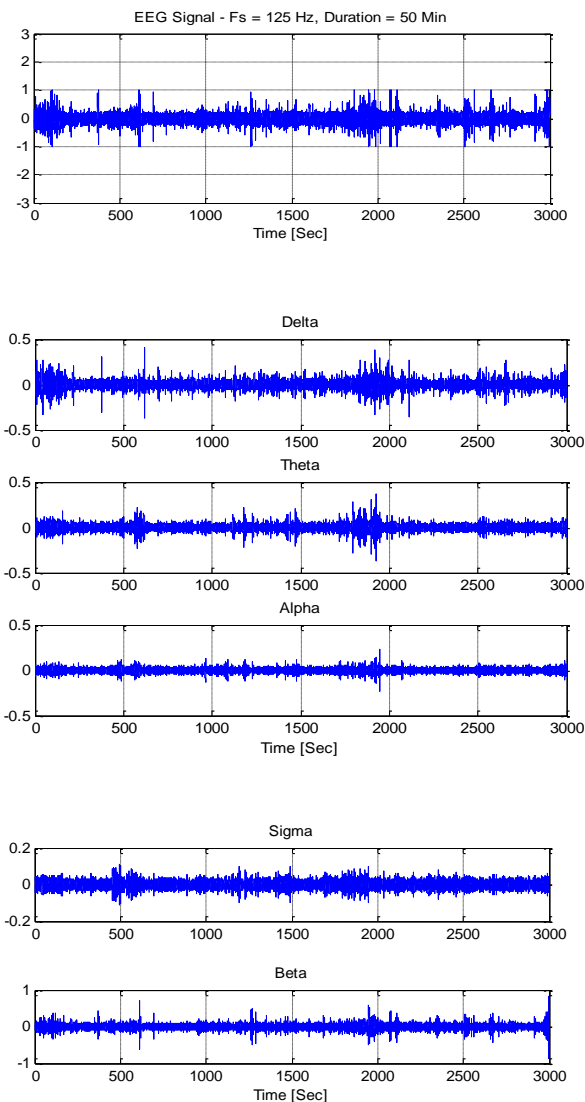


**Figure 3:** DWT decomposition and sub-band signal reconstruction

So the conclusion is that the automatic detection for the level of alertness of a moving subject (in our case it will be the driver) is difficult. This is because of following reasons [15] [16]:

- The spectral evolution of the density depends largely on the subject.
- STFT is very sensitive to artifacts caused by the subject's movements and blinking of the eyes.
- The minimum size of the window, ensuring sufficient accuracy of the FT, is not compatible with the short wave puff detection objective alpha.

In order to overcome these limitations, we evaluated other time analysis techniques frequency, such as the Hilbert Huang transform. The Hilbert Huang transform is a time-frequency analysis method introduced for the first time in 1998 by Norden E. Huang to calculate the time frequency energy distribution of any signal [17] [18]. This method consists of adaptively decomposing the signal into a sum of oscillating components which has a single frequency for each sample and then calculating the frequency and the instantaneous amplitude of each of these components using the Hilbert transform. The decomposition of the signal into mono-modal components is called Empirical Mode Decomposition (EMD).

Unlike the Fourier transform or wavelet transforms, the basis of decomposition of the EMD is specific to the signal. One of the motivations for the development of the EMD is the search for an estimate of the instantaneous frequency of the signal. Indeed, the classical approach of estimating the instantaneous frequency based on the Hilbert transform is strictly limited to the single component signals [19]. We will explain in more detail the two stages of the Hilbert Huang transform.

Let us take the difference between 3 samples ( $n + 1$ ,  $n$  and  $n - 1$ ) to calculate the frequency.

The EMD is a sifting process, allowing to decompose any multimodal signal into a sum of monomodal signals, called "intrinsic modes", or IMFs, for "Intrinsic Mode Functions". The decomposition is local, iterative, and fully data driven. The EMD deliberates the signals on the scale of their confined oscillations, without these being necessarily harmonic in the Fourier sense. The extraction of the IMFs is nonlinear, but their recombination for the exact reconstruction of the signal is linear. Based on the natural variations (or oscillations) of the signal, the EMD may allow an interpretation of the physical phenomena present in the signal [19].

### Intrinsic Mode Function (IMF)

It is a type of function that should fulfill two circumstances [19]:

1. Have a number of zero crossings and extrema equal to or at most different from one.
2. At all times, the average value between its lower and upper envelope must be zero.

The second condition is necessary for the instantaneous frequency to have no undesirable fluctuations due to signal asymmetry [19]. These two conditions ensure the uniqueness

of the oscillatory mode of the IMF at each moment. Figure presents an example of an IMF, extracted from an EEG. It can be verified that the no. of extrema is equal to the no. of passages by zero, as well as the proportion of the lower and upper envelope with respect to zero:

The signal  $x(t)$  as a finite combination of oscillations is expressed as:

$$X(t) = \sum_{i=1}^n IMF_i(t) + r(t) \quad (4)$$

Where  $n$  is the number of the IMFs and  $r(t)$  is the residue of the decomposition

The proposed approach relies entirely on the oscillatory characteristics of  $x(t)$ . This decomposition is entirely driven by the signal and adapted to it. This is why the name intrinsic modal function (IMF) has been used. After complete decomposition if all the IMFs and the residue, then reconstruct the original signal without loss or deformation of the initial information. The first step of the decomposition is to identify the local extrema. At that point interpolate all the maxima with a cubic spline to construct the upper envelope. Then same will be repeated for minima. The mean value of the lower and upper envelopes ( $m_1$ ) is then subtracted from the original signal  $X(t)$ .

$$X(t) - m_1 = h_1 \quad (5)$$

A stop criterion must be defined to ensure that the signal obtained verifies the properties of an IMF while limiting the number of iterations. The criterion proposed by Huang is based on the calculation of the relative variation of the signal between two consecutive iterations of the algorithm [19].

$$SD = \sum_{t=0}^T \frac{|(h_{1(k-1)}(t) - h_{1k}(t))|^2}{h_{1(k-1)}^2(t)} \quad (6)$$

Due to the decomposition method, this first IMF ( $c_1$ ) contains the high-frequency component of the signal. Subsequently, this component is deducted from the signal to calculate the first residue

$$r_1 = X(t) - c_1 \quad (7)$$

$r_1$  contains lower frequency components than  $c_1$  and will be processed using the same process that we have just described, to extract the 2<sup>nd</sup> IMF, and so on. Decomposition is stopped in step  $n$ , if at the termination of the decomposition, the expression of the original signal is given by:

$$X(t) = \sum_{i=1}^n c_i + r_n \quad (8)$$

EMD can summarize this method of decomposition with the following algorithm [19] [20]:

1. Copy the signal into an auxiliary variable  $h(t)$ .
2. Find the local extrema (maximum and minimum) of  $h(t)$ .

3. Compute the equation of the lower envelope (EnvMin(t)) and upper envelope (EnvMax(t)) of signal  $h(t)$  by the cubic spline method.
4. Then calculate the local average envelope:  $m(t) = 1/2 (EnvMin + EnvMax)$ .
5. Calculate the residue  $r(t)$  by subtracting the average envelope  $m(t)$  from the signal  $h(t)$ .
  - a. If the signal  $r(t)$  satisfies the properties of an IMF, then  $IMF_i = r(t)$ .
  - b. If not: repeat steps 2 to 5 with  $h(t) = r(t)$ .
6. The IMF thus determined is deducted from the original signal.
  - a. If the remainder has a sufficient number of extrema (greater than two), return to step 1 to fetch another IMF.
  - b. Otherwise, the residue is considered as the final residue  $r(t)$  of equation (4).

Ideally, the process of extracting the IMFs is completed when the residue no longer contains extrema. This means that the residue is a monotonic function that corresponds to the drift or the tendency of the initial signal.

### Modified Stop criterion

Now that we have seen how to calculate envelopes by minimizing errors, it remains to define a criterion to stop the iterations. In the theoretical part, we have seen that the standard deviation between two consecutive results of the algorithm can be constitute a stop criterion [equation (6)]. However, such a criterion does not peaks of high amplitude and short duration in the signal.

To avoid this kind of problems we have implemented a technique proposed by Flandrin et al. [20] and which consists in calculating the normalized average envelope:

$$m_{norm}(n) = 2 \frac{|m(n)|}{|EnvMax(n) - EnvMin(n)|} \quad (9)$$

And to stop the iterations when one of these two conditions is fulfilled:

- The percentage of points in the standardized average envelope exceeding one Value stop1 is greater than a stop 2.
- No point in the normalized average envelope is greater than stop2.

During the implementation, we chose Stop1 = 0.05, Stop2 = 0.5

### Change in the frequency Detection

To fit our way to deal with EEG signals, we speak to these signals as indicated by an extremely straightforward model:

$$y(t) = \sin(\varphi_0 + \varphi_1) + n(t) \quad (10)$$

Where  $\varphi_1$  is the angular frequency of the signal (corresponding to the frequency) and  $\varphi_0$  the stage,  $n(t)$  an enormous perturbation. The utilization of such a prototype is depended on the grounds that it doesn't signify the signal just within a small interval of time. The deviation of the frequency content is interpreted by the deviation of  $\varphi_1$ .

Consequently, we are occupied with evaluating it rapidly and online. The mathematical procedures are altogether shown. Keeping the continuous time nature of the flag we promptly watch that the noise-free signal  $x(t) = y(t) - n(t)$  attains the accompanying linear differential equation with constant coefficient:

$$\ddot{x}(t) + \varphi_1^2 x(t) = 0 \quad (11)$$

Converting equation (11) into operational domain:

$$s^2 x(s) - sx(0) - \dot{x}(0) + \varphi_1^2 x(s) = 0 \quad (12)$$

After calculating the preliminary state:

$$(s^2 + \varphi_1^2)x(s) = \varphi_1 \cos \varphi_0 + s \sin \varphi_0 \quad (13)$$

The parameter  $\varphi_1^2$  is then linearly detectable and at the moment its approximation is described. Taking double derivative with respect to  $s$  approves to overlook organized perturbations, here are the preliminary circumstances

$$2x + 4s \frac{dx}{ds} + (s^2 + \varphi_1^2) \frac{d^2x}{ds^2} = 0 \quad (14)$$

Then, we multiply both sides by  $s^{-2}$  to circumvent derivations with respect to time (positive power of  $s$ )

$$2s^{-3}x + 4s^{-2} \frac{dx}{ds} + (s^{-1} + s^{-3} \varphi_1^2) \frac{d^2x}{ds^2} = 0 \quad (15)$$

The eminent rule of operative calculus produces the subsequent on-line estimator of  $\varphi_1^2$ , i.e., a time-domain depiction with no derivative but only integrations with respect to time:

$$\varphi_1^2(t) = -2 \frac{\int_{t-T}^t ((T-\tau)^2 - 4(T-\tau)\tau + \tau^2)x(\tau) d\tau}{\int_{t-T}^t (T-\tau)^2 \tau^2 x(\tau) d\tau} \quad (16)$$

Give us a chance to take note of that the numerous integrals are changed in basic integrals with the assistance of Cauchy. In addition,  $T$  specifies the measure of sliding estimation window.

### Location of Alpha, Theta and High Frequency Waves

The first step of the analysis is to filter the EEG with a Butterworth filter tape 0.5-25 Hz, to remove high-frequency components that do not information about arousal and that may interfere with us during the increase the number of iterations in the EMD.

- The difference in EEG amplitudes between subjects led us to normalize the signal by dividing it by its standard deviation, in order to be able to set the thresholds valid whatever the subject. This amounts to customizing the analysis.

- Then we apply the Hilbert-Huang transform on the filtered and normalized signal, and thus obtain a set of IMFs as well as their instantaneous amplitude and frequency.

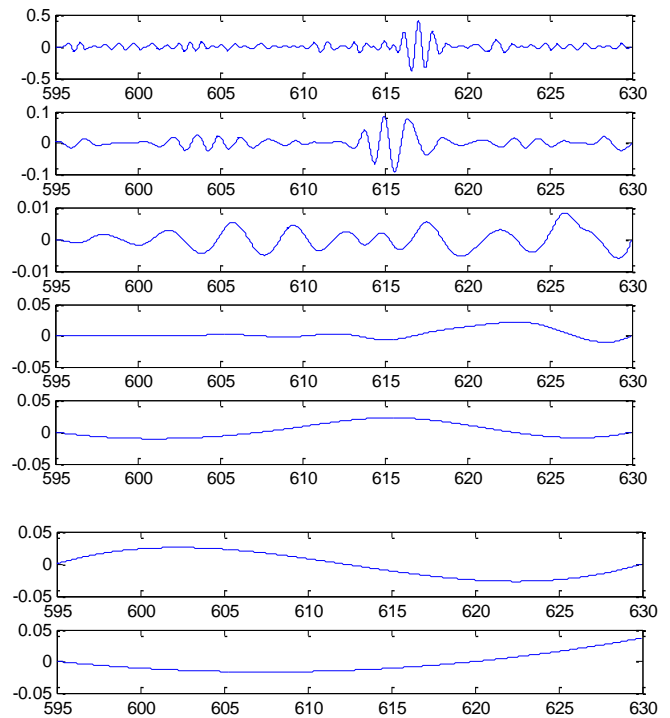


Figure 5: HHT of delta waves

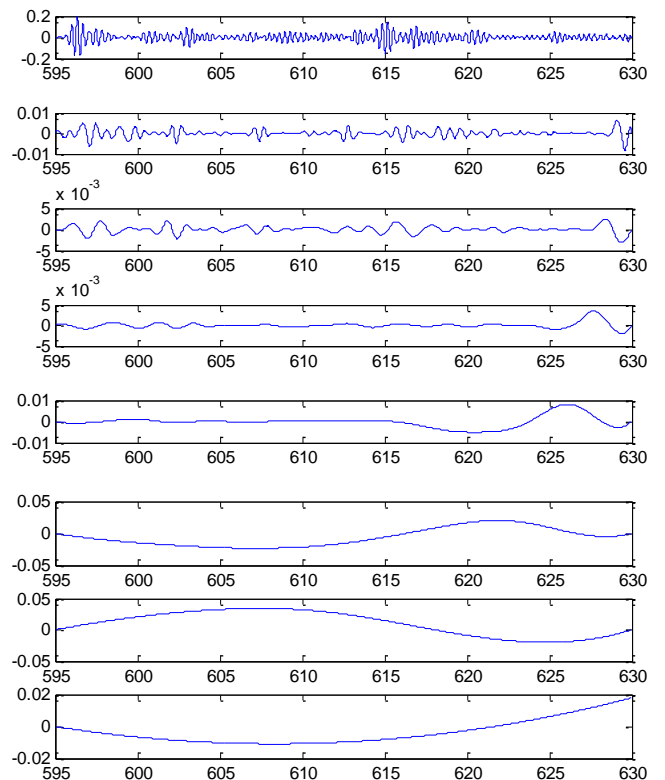


Figure 6: HHT of Theta

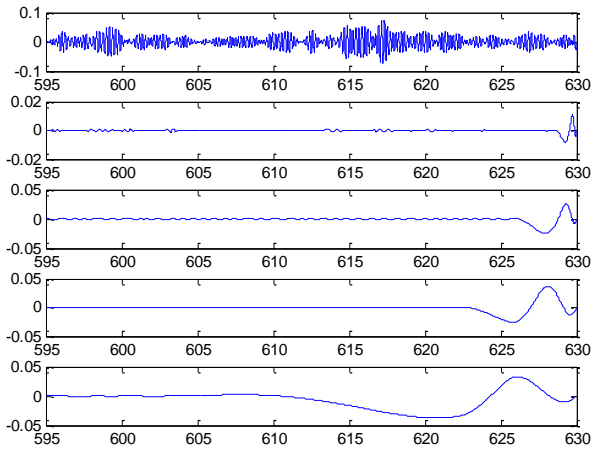


Figure 7: HHT of Alfa

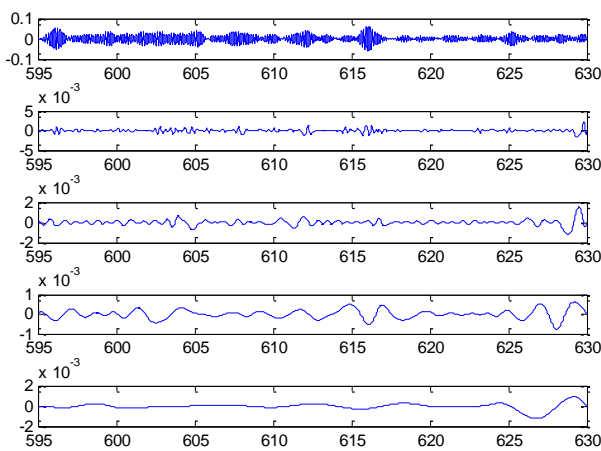


Figure 8: HHT of sigma

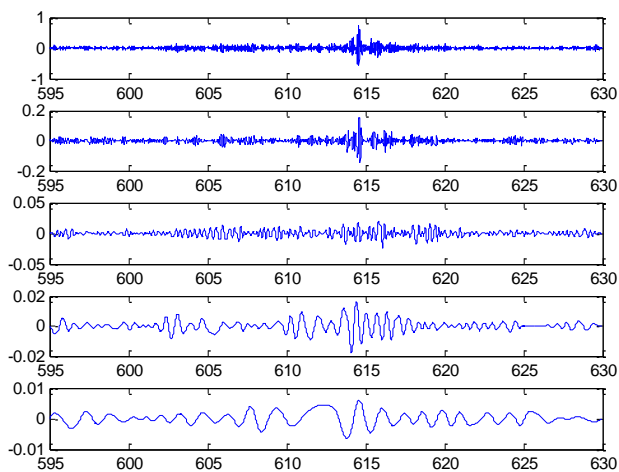


Figure 9: HHT of beta

- After we read the instantaneous frequency of each IMF by calculating the average on a sliding window of  $N$  points centered on the current point:

$$x_{filters}[n] = \frac{1}{N} \sum_{i=n-N/2}^{n+N/2} x[i], n = \left[ \frac{N}{2}, \dots, L - \frac{N}{2} \right] \quad (17)$$

Where  $L$  is the length of the sequence considered. In practice, we have chosen  $N$  that the mean is calculated on 0.125 s.

This filter, which reduces calculation errors, is necessary to avoid discontinuities in subsequent stages. The next step is to locate the waves that interest us. For each IMF, the sequences whose instantaneous frequency is and we recombine them to keep, in the end, only the part of the signal containing the selected frequencies. This is equivalent to using the HHT such as a bandpass filter. In the next sub sections we compare the performance of such an approach with those of a more conventional filtering.

At the end of this step we will have three signals, each giving the contribution of the signal original in the studied bands. By applying the Hilbert transform, we compute, for each instant, the amplitudes of these components, which we will denote respectively by  $A_\alpha$ ,  $A_\theta$  and  $A_{HF}$ , in the band  $\alpha$ ,  $\theta$  and the high frequencies. Now it remains to identify, with each sample, the frequency band which predominates..

### Block Diagram of the Analysis Process

The diagrams below represent the EEG analysis method and the proposed method in order to try to reproduce the visual analysis of the expert to locate the waves  $\alpha$  and  $\theta$ .

EEG arousal annotation has been given in dataset, and considered as ground truth. We have extracted the information about arousal index form dataset for 8 hour samples. The extracted information is stored in separate database as features. Few portion of the features is considered as training information to SVM. Further SVM is trained as knowledge of Arousal frequencies, different test is sampled to test the SVM model for Arousal detection

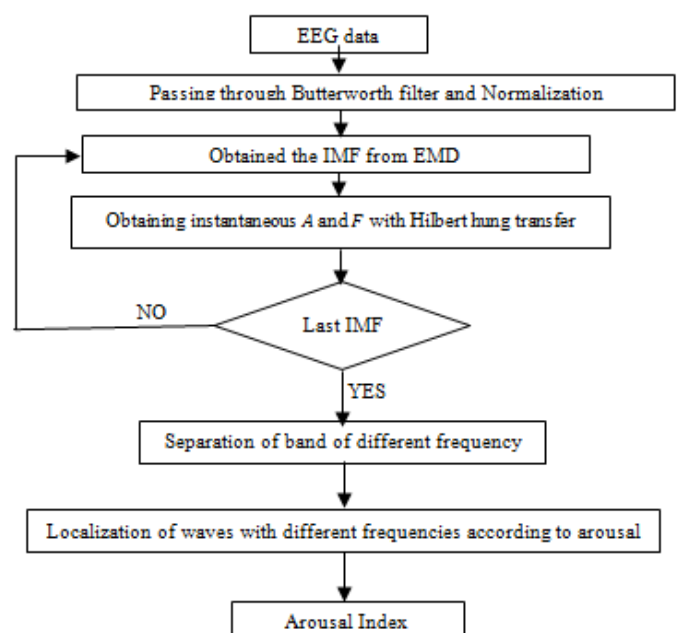
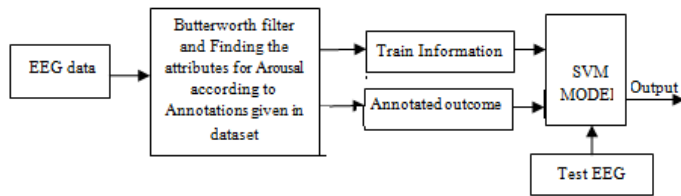


Figure 10: EEG analysis for arousal detection



**Figure 11:** Arousal index detection using SVM classifier based on annotations

**Generalities on Support Vector Machines**

Indeed, the main objective of SVM applied to the recognition of forms is to construct an optimal separating hyperplane between two classes, i.e., with the largest margin, right Figure 12. When a linear solution is not possible, the method realizes a projection of the input space X in a space of characteristics Z of larger size, through a function  $\phi(x)$ , Figure 12(a). An example of this type of function is the internal product, estimated through kernel functions:

$$\phi(x_1)^T \phi(x_2) = (z_1^T z_2) = \sum_{r=1}^m a_r z_r(x_1) z_r(x_2) \Leftrightarrow k(x_1, x_2), \forall a_r \geq 0 \tag{18}$$

Satisfying the conditions of Mercer [19], like the Gaussian kernel:

$$k(x_i, x_j) = \exp \left[ -\frac{(x_i - x_j)^2}{2\sigma^2} \right] \tag{19}$$

Therefore, appreciations to the autonomy to utilize various types of kernel, the optimal separator hyperplane resembles to various nonlinear estimators in the original space, Figure 12 (b).

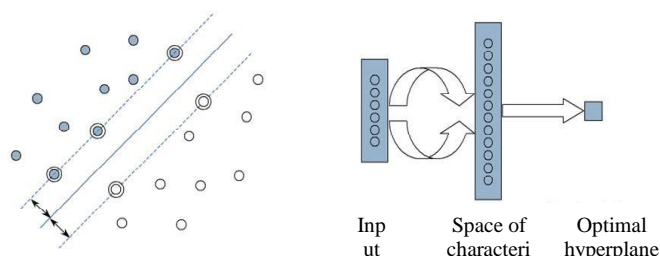


**Figure 12 (a)** Optimal separator hyperplane with surrounded support vectors **(b)** Transformation of the input space into a space of characteristics of greater dimension

In traditional learning machines, particularly neural networks, the search for the architecture of the determination of its parameters is decoupled; it is necessary to look for the parameters of several structures in order to choose the one that guarantees the best power of generalization. This involves

partitioning the database into a learning database and a test database. For SVM, this research is no longer necessary; one can use the entire database and the approach ensures, mathematically, the best architecture.

For reasons of simplicity, we will describe the SVM applied only to the classification, since the formulations for the regression and density estimation problems have a form very similar to that of the classification.

**SVM Applied to Classification**

Suppose that the training set  $\{x_1, y_1\}, \dots, \{x_\ell, y_\ell\}$ , where  $x \in X$  and  $y \in \{-1, 1\}$ , where  $\ell$  is the number of observations and X is a distribution in space  $\mathfrak{R}^n$ . In the classification problem, the goal is to find an efficient method to construct the optimal separator hyperplane, i.e., with the greatest margin. To do this, one must find the vector  $w$  and the constant  $b$ , which minimize the norm  $|w|^2 = w^T w$  (since it is inversely proportional to the margin), under the constraints:

$$w^T x_i + b \geq 1, \quad \text{if } y_i = 1 \tag{20}$$

$$w^T x_i + b \leq -1, \quad \text{if } y_i = -1 \tag{21}$$

Because one can accept some errors, one relaxes the constraints (21) & (22) and introduces an additional cost related to this relaxation, so that one arrives at the quadratic problem, QP, following:

$$\text{Minimize} \quad \frac{1}{2} (w^T w) + C [\sum_{i=1}^{\ell} \xi_i]$$

$w$

Under the constraints  $y_i (w_i^T x + b) \geq 1 - \xi_i$ ,

$$\xi_i \geq 0 \quad i = 1, \dots, \ell \tag{22}$$

The problem (22) can be solved in the primal space (the space of parameters  $w$  and  $b$ ). In fact, one solves the QP in the dual space, equation (23), (the Lagrange multiplier space) for two main reasons: 1) The constraints (21) and (22) are replaced by the associated Lagrange multipliers, and 2) We obtain a formulation of the problem where the training data appear as an internal product between vectors, which can then be replaced by kernel functions, then construct the hyperplane in the feature space and obtain functions Non-linear in the input space.

Maximize

$$L_D(\alpha) = \sum_{i=1}^{\ell} \alpha_i - \frac{1}{2} \sum_{i,j=1}^{\ell} \alpha_i \alpha_j y_i y_j (x_i^T x_j)$$

$\alpha$

Under the constraints  $\sum_{i=1}^{\ell} y_i \alpha_i = 0$ ,  
 $0 \leq \alpha_i \leq C \quad i = 1, \dots, \ell$

(23)

Where,  $\alpha_i$  is the Lagrange multiplier, associated with constraints. Parameter  $C$  controls the level of error in the classification.



The SVM evaluation function is defined as:

$$f(x) = \sum_{i=1}^l \alpha_i y_i k(x_i, x) + b \quad (24)$$

The examples  $x_i$  associated with the Lagrange multipliers  $\alpha_i$  larger than zero correspond to the support vectors, and have a significant contribution to equation (24). Geometrically, these vectors reside in the margin defined by the separating hyperplane. The constant  $b$  represents the threshold of the hyperplane learned in the characteristic space. It can be calculated by the mean of the function (24), evaluated using the support vectors.

## EXPERIMENTAL PROCEDURE

### Database

The experiments conducted in this work use different data sets containing PSG recordings from real patients. All recordings were taken from the Sleep Heart Health Study (SHHS) [21], a database granted by the Case Western Reserve University, emerged from a multicenter cohort study implemented by the National Heart Lung and Blood Institute to determine the cardiovascular and other consequences of sleep-disordered breathing. Each recording includes the annotations of different events, including EEG arousals, marked in annotation.txt file in database given in [22]. Polysomnograms were acquired in an unattended setting, as a rule in the homes of the members, via prepared and guaranteed professionals. The recording montage comprised of: C3/A2 and C4/A1 EEGs, inspected at 125 Hz, right and left electrooculograms (EOGs), tested at 50 Hz, a bipolar submental EMG, examined at 125 Hz, thoracic and abdominal excursions (THOR and ABDO), "wind stream", fingertip beat oximetry (Nonin, Minneapolis, MN), Heart rate (PR), body position (utilizing a mercury gage sensor), encompassing light. Eight hours recording dataset has been taken and 31069 samples are taken, where total observed detected arousal was 89. The experiment has been conducted in two ways one is machine learning approach and the other is threshold based prototype given by SHHS for arousal indexing.

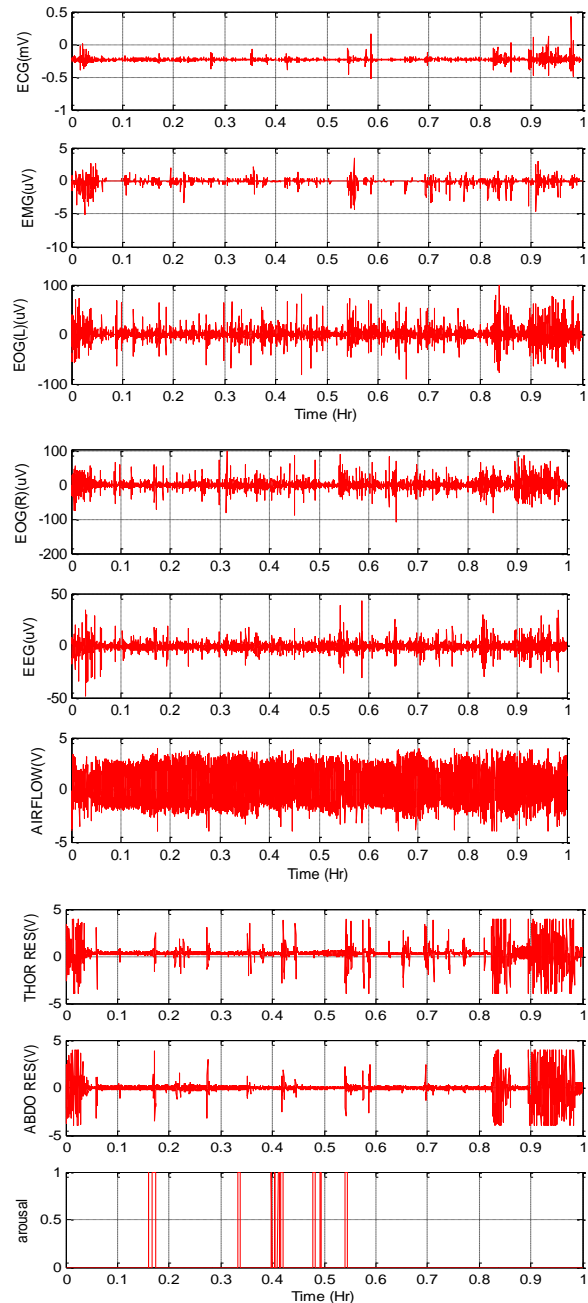
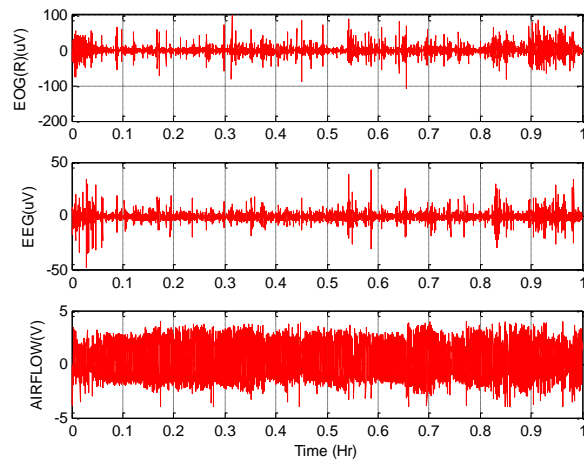


Figure 13: EEG database plot



### Performance Evaluation Parameter

$$\text{Accuracy} = \frac{TP+TN}{TP+TN+FP+FN} \times 100$$

$$\text{False Negative Rate} = \frac{FN}{FN+TP} \times 100$$

$$\text{False Positive Rate} = \frac{FP}{FP+TN} \times 100$$

Where, TP=True Positive

TN=True Negative

FP=False Positive

FN=False Negative

### SIMULATION RESULTS

This section presents a detailed display of result for single arousal. Figure below shows the EEG wave for arousal which occurred on T = 602 sec and lasted for approximately 27 sec. change in frequency and amplitude is clearly visible.

To detect arousal we first applied DWT and separated different bands of wave as shown below. As inspected visibly this bands give useful information, significant change in amplitude delta and beta waves and change in instantaneous frequency of theta and alpha waves. As the arousal starts at T = 602 sec, we can see in the EEG signal that its frequency increases (can be seen in above figure, after T = 602s signal get denser) this change directly reflects in change of frequency and amplitude of alpha waves.

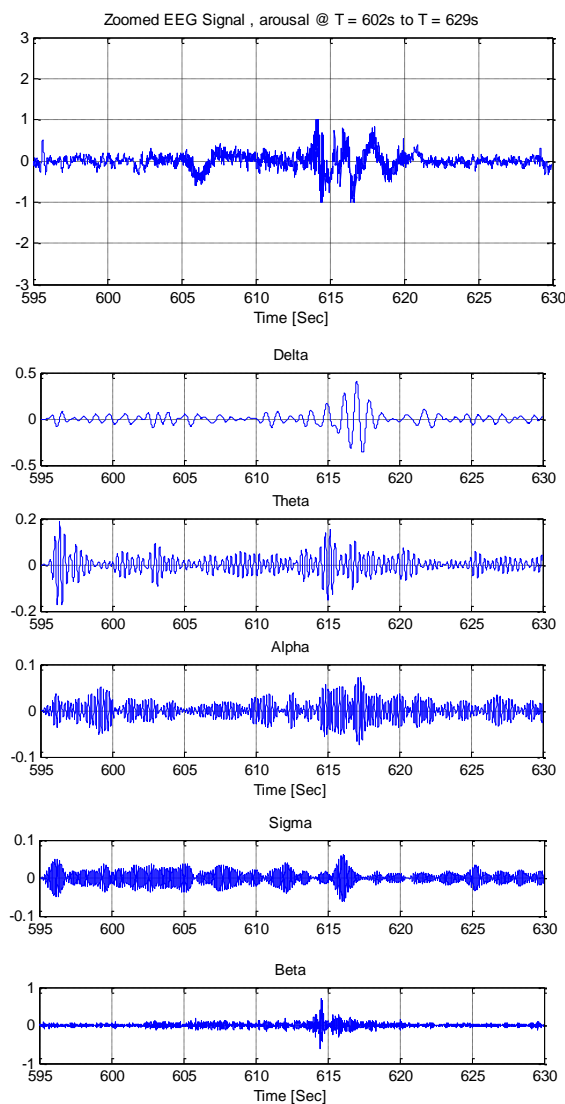


Figure 14: Zoomed EEG signal

Theta waves also produces abruptly changing envelopes. Beta waves generally shows low amplitude during sleep but during

arousal amplitude of beta waves also increases. Delta wave does not show significant frequency change but change in amplitude can be interpreted as change in breathing or body movement.

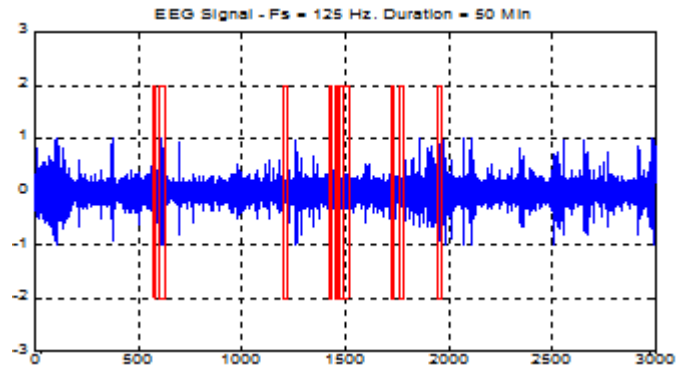


Figure 15: Final arousal detection with frequency change detection

Figure 15 shows detected arousal for EEG signal marked red. This detections nearly matches with the ground truth, Shown in table 1.

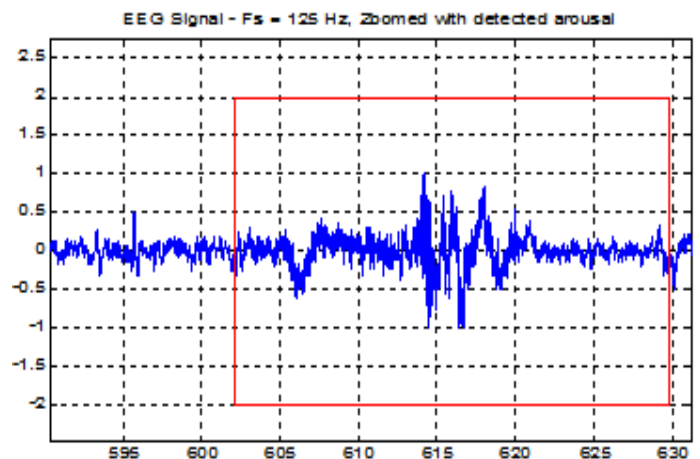


Figure 16: EEG zoomed signal with detected arousal

Figure 16 is the zoomed version of Figure 15. Arousal is detected by the frequency change in alpha, beta, delta, theta and sigma waves. False detections are ruled out using the criteria that an arousal is the abrupt change in frequency after 10 second of sleep and lasts more than 3 seconds.

### EXPERIMENTAL RESULTS

Accuracy=90.4444%

False Negative Rate=42.6471

False Positive Rate=8.2564

**Table 1:** Comparison of result with ground truth information of arousal

Time	Sample	Ground truth for arousal detection	Arousal Detection using Proposed Method
[21:39:35.000]	575	Arousal 0:06.3	Arousal 0:05.1
[21:40:02.000]	602	Arousal 0:27.8	Arousal 0:25.4
[21:50:00.000]	1200	Arousal 0:17.1	Arousal 0:18.5
[21:53:50.000]	1430	Arousal 0:06.4	Arousal 0:04.9
[21:54:15.000]	1455	Arousal 0:04.2	Arousal 0:03.8
[21:54:38.000]	1478	Arousal 0:08.7	Arousal 0:07.3
[21:54:58.000]	1498	Arousal 0:16.3	Arousal 0:15.5
[21:58:45.000]	1725	Arousal 0:14.9	Arousal 0:13.2
[21:59:29.000]	1769	Arousal 0:13.8	Arousal 0:12.4
[22:02:23.000]	1943	Arousal 0:21.1	Arousal 0:19.8
[22:38:09.000]	4089	Arousal 0:03.2	Arousal 0:04.6
[22:39:59.000]	4199	Arousal 0:11.1	Arousal 0:10.3
[22:41:25.000]	4285	Arousal 0:06.2	Arousal 0:05.8
[22:42:33.000]	4353	Arousal 0:05.6	Arousal 0:04.1
[22:45:07.000]	4507	Arousal 0:04.5	Arousal 0:03.6
[23:24:23.000]	6863	Arousal 0:07.8	Arousal 0:06.9
[23:25:40.000]	6940	Arousal 0:04.3	Arousal 0:03.7
[23:28:39.000]	7119	Arousal 0:03.3	Arousal 0:04.1
[23:30:54.000]	7254	Arousal 0:04.0	Arousal 0:03.8
[23:31:35.000]	7295	Arousal 0:10.0	Arousal 0:10.5
[23:32:35.000]	7355	Arousal 0:07.0	Arousal 0:6.3
[23:33:14.000]	7394	Arousal 0:04.3	Arousal 0:03.8
[23:34:55.000]	7495	Arousal 0:13.0	Arousal 0:13.6
[23:35:31.000]	7531	Arousal 0:07.3	Arousal 0:06.1
[23:36:33.000]	7593	Arousal 0:07.2	Arousal 0:06.6
[23:38:55.000]	7735	Arousal 0:11.8	Arousal 0:10.4
[23:40:28.000]	7828	Arousal 0:03.1	Arousal 0:02.5
[23:41:51.000]	7911	Arousal 0:04.2	Arousal 0:04.8
[23:54:45.000]	8685	Arousal 0:04.7	Arousal 0:03.0

## CONCLUSION

EEG arousals cause sleep fragmentation, one of the primary reasons why a decent night's sleep is impossible for patients with a high arousal index. The detection of these events is mandatory for a correct and complete analysis of a PSG recording and, thus, for the diagnosis of sleep disorders. This complex task implies the analysis of multiple signals at the same time, being also time-consuming for the expert. To solve the inherent problems associated to this task, the time an expert needs and the subjectivity associated to the process, an automatic method is desired. This paper attempts to solve the

problem proposing a new technique for the automatic detection of EEG arousals using feature based and SVM classifier. The other novel method is based on frequency change estimation for arousal detection. The outcome is compared with ground truth and outcome is satisfactory. Previous research work [23] attained 86% accuracy while the proposed approach reaches 90.44% accuracy

## REFERENCES

- [1] Berry, R.B., Brooks, R., Gamaldo, C.E., Harding, S.M., Marcus, C.L. and Vaughn, B.V., "The AASM manual for the scoring of sleep and associated events". "Rules, Terminology and Technical Specifications, Darien, Illinois, American Academy of Sleep Medicine", 2012.
- [2] Álvarez-Estévez, D. and Moret-Bonillo, V., "Identification of electroencephalographic arousals in multichannel sleep recordings". IEEE Trans. on Biomedical Engineering, vol. 58, pp.54-63, 2011.
- [3] ASDA, E., "arousals: scoring rules and examples: a preliminary report from the Sleep Disorders Atlas Task Force of the American Sleep Disorders Association". Sleep, vol. 15(2), pp.173-184 1992.
- [4] Rechtschaffen, A. and Kales, A., "A manual of standardized terminology, techniques, and scoring systems for sleep stages of human subjects", 1968.
- [5] Karmakar, C., Khandoker, A., Penzel, T., Schobel, C. and Palaniswami, M., "Detection of respiratory arousals using photoplethysmography (PPG) signal in sleep apnea patients". IEEE journal of biomedical and health informatics, vol. 18(3), pp.1065-1073, 2014.
- [6] Wallant, C.T., Chellappa, S.L., Gaggioni, G., Jaspard, M., Meyer, C., Muto, V., Vandewalle, G., MAQUET, P. and Phillips, C., "Automatic artifact detection for whole-night polysomnographic sleep recordings", 2014.
- [7] Mensen, A., Riedner, B. and Tononi, G., "Optimizing detection and analysis of slow waves in sleep EEG". Journal of neuroscience methods, 274, pp.1-12, 2016.
- [8] Fernández-Varela, I., Hernández-Pereira, E., Álvarez-Estévez, D. and Moret-Bonillo, V., "Combining machine learning models for the automatic detection of EEG arousals". Neurocomputing, 2017.
- [9] Giralt, A., "Driver hypovigilance criteria, filter and HDM module". AWAKE Deliverable, 3, 2003.
- [10] Åkerstedt, T., Peters, B., Anund, A. and Kecklund, G., "Impaired alertness and performance driving home from the night shift: a driving simulator study". Journal of sleep research, vol. 14(1), pp.17-20, 2005.
- [11] Matteo Frigo, Steven G. Johnson, [www.fftw.org](http://www.fftw.org), "Fast Fourier Transform in the West", MIT.

- [12] Weiss, G. ed., "Multiagent systems: a modern approach to distributed artificial intelligence". MIT press, 1999.
- [13] Bekiaris, E. and Nikolaou, S., "State of the art on driver hypovigilance monitoring and warning systems". AWAKE (System for effective Assessment of driver vigilance and Warning According to traffic risk Estimation) ISSN:2000-28062, 2002.
- [14] Graps, A., "An introduction to wavelets". IEEE computational science and engineering, vol. 2(2), pp.50-61, 1995.
- [15] Jammes, B., Sharabaty, H. and Estève, D., "Alpha and Theta wave localization" in EEG signals: Survey of Existing algorithms. SENSATION IST507231, Document ID: Sens-LAAS-A, 2005..
- [16] Jammes, B. and SHARABATY, H., "Criteria for sleep and stress detection and data feature extraction algorithms". SP4-WP4. 4-A4. 4.1 Project 1ST SENSATION N° 507231, 2006.
- [17] Huang, N.E., "Hilbert-Huang transform and its applications", World Scientific, Vol. 16, 2014.
- [18] Huang, N.E., Shen, Z., Long, S.R., Wu, M.C., Shih, H.H., Zheng, Q., Yen, N.C., Tung, C.C. and Liu, H.H., "The empirical mode decomposition and the Hilbert spectrum for nonlinear and non-stationary time series analysis". In Proceedings of the Royal Society of London A: mathematical, physical and engineering sciences. The Royal Society, Vol. 454, No. 1971, pp. 903-995, 1998
- [19] Cexus, J.C. and Boudraa, A.O. "Nonstationary signals analysis by Teager-Huang transform (THT)". Signal Processing Conference, 2006 14th European , pp. 1-5, IEEE, 2006.
- [20] Rilling, G., Flandrin, P. and Goncalves, P. "On empirical mode decomposition and its algorithm"s. In IEEE-EURASIP workshop on "nonlinear signal and image processing ", Vol. 3, pp. 8-11. IEEE, Grado, Italy, 2003.
- [21] Sleep Heart Health Study (SHHS) dataset, Online available at: <https://sleepdata.org/datasets/shhs>
- [22] SHHS PSG Database, Online available at: <https://physionet.org/pn3/shhpsgdb/>
- [23] Sugi, T., Kawana, F. and Nakamura, M., "Automatic EEG arousal detection for sleep apnea syndrome". Biomedical Signal Processing and Control, vol. 4(4), pp.329-337, 2009.